

PETROLOGY AND MINERALOGY OF WINONAITE NORTHWEST AFRICA (NWA) 14988. Zilong Wang^{1,2}, Wei Tian¹, Ao Su¹, and Wei-(RZ) Wang². ¹School of Earth and Space Sciences, Peking University, Beijing 100871, China [zilong.wang@pku.edu.cn; davidtian@pku.edu.cn], ²Key Laboratory of Paleomagnetism and Tectonic Reconstruction of MNR, Institute of Geomechanics, Chinese Academy of Geological Sciences, Beijing 100871, China.

Introduction: The winonaites are a meteorite group of primitive achondrites formed from partial-melting residues of a chondritic precursor. They show highly reduced mineral compositions and the oxygen three isotopic compositions ($\Delta^{17}\text{O}$) identical to IAB irons, suggesting that winonaites and IAB groups share the same parent body [1–3]. To date, 86 meteorites have been classified as winonaites (Meteoritical Bulletin Database, accessed on 21st December 2023), and more than half of the numbers were discovered after 2018. However, only a minority of them have been investigated in detail. This study reports preliminary petrographic and mineralogical results of a newly discovered winonaite, NWA 14988, to shed new insights into the diversity of this meteorite group.

Results: The mineral modal abundances of NWA 14988 (Fig. 1) are: orthopyroxene (50.4%), olivine (17.9%), plagioclase (16.8%), Fe oxides (8.1%), troilite (2.8%), clinopyroxene (2.6%), kamacite (0.4%), taenite (0.4%), chromite (0.2%), calcite (0.2%), K-feldspar (0.1%), schreibersite (0.1%), and phosphate (merrillite, 0.1%) (Fig. 1). This meteorite is moderately weathered, with the occurrence of Fe oxides and calcite consistent with the hot desert environment [4].

Petrology. The silicate minerals generally exhibit a grain size range of 100–250 μm , which is typical for winonaites. These minerals exhibit an equigranular texture with abundant 120° triple junctions, suggestive of slow-cooling equilibrium condition deep within the interior of its parent body (Fig. 2). The gross metal content (9.0 vol.%) is lower than most of the reported winonaites (~8–32 vol.%), while the plagioclase abundance (16.8%) is higher than them (~3–17 vol.%) [5]. No chondrules are present in the analyzed slice. Representative Raman spectra of the minerals are shown in Fig. 3.

Mineralogy. The compositions of silicate minerals are rather homogeneous, again indicative of chemical equilibrium. The Mg# of olivine, orthopyroxene, and clinopyroxene ranges from 98.5–98.9, 95.1–95.3, and 95.6–96.4, respectively (Table 1), similar to winonaites previously reported [6]. The plagioclase is sodic, with a composition of $\text{An}_{11.8-15.7}\text{Ab}_{79.7-83.7}\text{Or}_{4.1-4.9}$ and less varied compared to other reported winonaites.

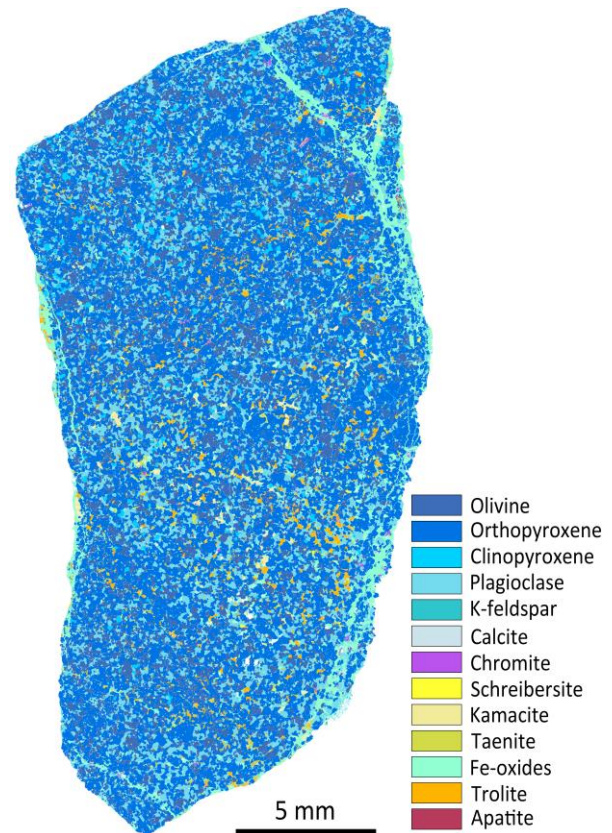


Fig. 1. Mineral modal-abundance map of NWA 14988.

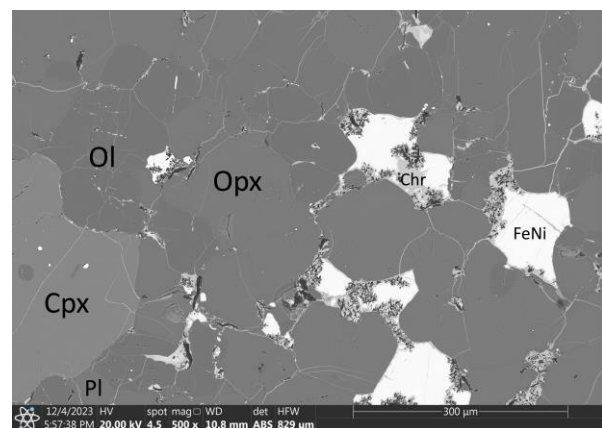


Fig. 2. Backscattered image of a local area in NWA 14988. Cpx = clinopyroxene, Opx = orthopyroxene, Ol = olivine, Chr = chromite, FeNi = FeNi metal.

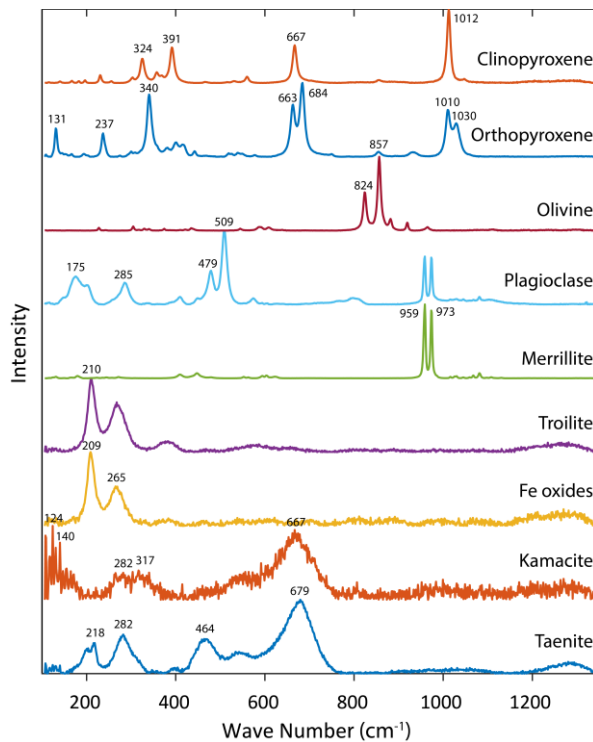


Fig. 3. Representative Raman spectra of minerals in NWA 14988.

Bulk chemistry. The bulk-silicate major-element composition of NWA 14988 is reconstructed based on the mineral model abundances and their average compositions. The reconstruction result is (in wt.%): SiO_2 55.71 ± 0.35 , TiO_2 0.16 ± 0.04 , Al_2O_3 3.44 ± 0.06 , Cr_2O_3 0.43 ± 0.04 , FeO 2.23 ± 0.09 , MnO 0.51 ± 0.03 , NiO 0.04 ± 0.01 , MgO 33.86 ± 0.21 , CaO 1.87 ± 0.12 , Na_2O 1.34 ± 0.09 , K_2O 0.11 ± 0.01 .

Table 1. Representative electron microprobe (EMP) compositions of major silicate phases in NWA 14988.

	Ol (n = 6)		Opx (n = 14)		Cpx (n = 5)		Pl (n = 6)		Chr (n = 1)
	Avg.	Std.	Avg.	Std.	Avg.	Std.	Avg.	Std.	
SiO_2	42.34	0.26	58.32	0.31	54.26	0.35	66.7	0.63	0.05
TiO_2	0.02	0.02	0.21	0.04	0.7	0.04	0.06	0.04	0.49
Al_2O_3	0	0	0.26	0.01	0.77	0.01	21.2	0.37	4.25
Cr_2O_3	0.04	0.03	0.3	0.04	1.5	0.13	0.02	0.02	66.68
FeO	1.27	0.18	3.2	0.06	1.32	0.14	0.18	0.09	0
MnO	0.22	0.04	0.71	0.03	0.42	0.06	0.02	0.01	10.5
NiO	0.02	0.03	0.02	0.01	0.02	0.02	0.01	0.01	6
MgO	55.62	0.18	35.45	0.27	17.88	0.17	0.01	0.01	9.81
CaO	0.04	0.01	1.17	0.09	22.28	0.38	2.55	0.31	0.03
Na_2O	0.02	0.02	0.04	0.02	0.8	0.03	8.4	0.47	0
K_2O	0	0	0.01	0.01	0	0.01	0.7	0.05	0
Total	99.58	0.21	99.67	0.39	99.96	0.52	99.85	0.49	97.81

Discussions: Although the modal abundances and mineral compositions of NWA 14988 are within the typical range of winonaite, they do not match any specific winonaite samples previously reported. This indicates that NWA 14988 is a unique component of

the interior of the winonaite-IAB parent body. Previous studies have also revealed the decimeter-scale heterogeneity of winonaite and IAB meteorites [7], suggesting that the unpaired characteristics observed in winonaite samples are likely inherited from their parent body. These findings suggest that the winonaite-IAB parent body was relatively small in size and exhibited heterogeneous heat distribution within its interior [8].

The equilibrium temperature (at 0 kbar) between clinopyroxene and orthopyroxene is calculated to be 926–941 °C using Thermobar [9]. This temperature range is close to the eutectic point (950 °C) of FeNi-FeS alloy, but remarkably lower than the onset temperature of silicate partial melting (~1100 °C, [10]) and falls at the lower end of two-pyroxene equilibrium temperatures recorded in most winonaite (900–1200 °C, [5]). These observations suggest that the silicates in the sample underwent very limited partial melting (<5 vol%) or did not melt at all. Alternatively, it is possible that the cooling rate was sufficiently low to allow elemental exchange between the clinopyroxene and orthopyroxene. Considering the homogeneous compositions of silicate minerals and the relative enrichment of plagioclase, the former explanation is more plausible. Therefore, NWA 14988 likely represents the upper-mantle lithology of winonaite-IAB parent asteroid. The calculated bulk Mg/Si (0.51) and Ca/Si (0.03) of NWA 14988 are inconsistent with any previously reported chondrite groups [11], suggesting that the winonaite-IAB parent body is distinct from the parent bodies of chondrites and has already been destroyed by cataclysmic impacts in the early solar system.

Acknowledgments: We thank Ziyao Wang for providing the meteorite sample, and Hongrui Ding for conducting the spectral analysis. This research is financially supported by the National Natural Science Foundation of China (No. 42272348).

References: [1] Clayton R. N. and Mayeda T. K. (1996) *GCA*, 60, 1999–2017. [2] Benedix G. K. et al. (1998) *GCA*, 62, 2535–2553. [3] Greenwood R. C. et al. (2012) *GCA*, 94, 146–163. [4] Koike M. et al. (2023) *86th AMMS*, 6177. [5] Zeng X. J. et al. (2019) *EPS*, 71, 38. [6] Mittlefehldt D. W. (2014) *Treatise on Geochemistry, Volume 1*, 235–266. [7] Mittlefehldt D. W. (1998) *RiMG*, 36, 4-01–4-196. [8] Hunt A. C. (2017) *GCA*, 199, 13–30. [9] Wieser P. E. (2022) *Volcanica*, 5, 349–384. [10] Ford R. L. et al. (2008) *Meteoritics & Planet. Sci.*, 43, 1399–1414. [11] Sears D. W. G. (2004) *The origin of chondrules and chondrites. Chapter 1*, 14.